URSI - RCRS 2022, IIT (Indore), India, 1 - 4 December, 2022

Investigating the Performance Benefits of Vectorized NavIC Receiver over Federated NavIC Receiver in Semi-Urban Environments

Abhijit Dey* (1), and Nitin Sharma (1)
(1) Department of Electrical and Electronics Engineering, Birla Institute of Technology and Science, Pilani, K.K. Birla Goa Campus, Goa, 403726, Email: abhijitdey89@gmail.com

Abstract

The Navigation with Indian Constellation (NavIC) system has created new opportunities for precise positioning across the Indian subcontinent. NavIC receivers are widely used for different applications, including in the autonomous vehicle industry. However, the performance and robustness of these receivers are contingent on satellite geometry, receiver architecture, and navigation environment. In semi-urban canyons with a high probability of signal blockage and/or interference from one or more satellites, scalar tracking (ST)-based NavIC receivers' positioning accuracy degrades. Vector tracking (VT)-based NavIC receivers, on the other hand, display some tolerance to transient outages and interference. Therefore, it is necessary to investigate VT-based NavIC receivers for various applications, particularly safety-critical applications. This study compares a single-frequency (L5/S) vectorized and federated NavIC software receiver in semi-urban environments.

1. Introduction

India's Navigation with Indian Constellation (NavIC) system has emerged and become a ubiquitous system capable of providing precise and accurate navigation and timing solutions in India and its near boundaries [1]. NavIC is being utilized in numerous applications, including transportation, agriculture, healthcare, autonomous vehicle navigation, etc [2]. Many of these applications involve safety- and liability-critical requirements. However, the positioning accuracy and reliability of the navigation solutions depend significantly on the availability and quality of the received signal. Recent studies have reported that the NavIC S-band signals are affected by the 2.45 GHz industrial, scientific and medical (ISM) radio bands [3]. Moreover, the receiver architecture also plays a significant role in the accuracy of navigation solutions. Most receivers employ conventional scalar tracking (ST)-based architecture. In ST, the signal tracking and navigation work independently and do not share any mutual information among the channels. On the other hand, vector tracking (VT) is a promising approach, where the satellite signals are tracked by a common Kalman filter-based navigation filter that combines the tasks of tracking and navigation into a single algorithm [4]. This enables remarkable enhancement in the robustness of the receiver in high dynamics and improves the sensitivity against weak signal reception. The widespread use and demand for accurate and robust navigation solutions for different NavIC-based applications have led to the need for reliable and robust receiver architecture for NavIC, which was the primary motivation for this research. In this regard, VT-based NavIC receivers are these days of great interest. The author's previous publication [5] presents the VT-based NavIC receiver for S-band interference. Later the dual-frequency VT-based architecture was presented in [6]. However, to the best of the author's knowledge, a comparison study on the performance benefits of VT over ST for NavIC has not been reported yet. This paper investigates the performance of a single-frequency scalar- and vector-based NavIC software receiver in semi-urban environments to provide robust, consistent, and reliable performance. The performance is evaluated for both L5 and S NavIC signals in semi-urban and clear open-sky areas. In one case, the signals are potentially affected by the high dynamics, signal attenuation, and interference, while in another, direct line-of-sight (LOS) signals were received in high dynamics. The rest of the paper is structured as follows. Section 2 describes the NavIC receiver architecture implementation based on ST and VT. Section 3 illustrates the experimental setup and scenarios. The detailed performance evaluation results are presented and discussed in Section 4. Finally, Section 5 concludes this paper.

2. NavIC Software Receiver Implementation Approaches

The conventional ST-based or federated and vectorized receiver architecture of the NavIC software receiver are explained in this section. The block schematic of the implemented NavIC software receiver is shown in Fig. 1.

(a) Scalar Tracking or Federated NavIC software receiver architecture

In the federated form of architecture, the receiver employs the conventional ST loops for code and carrier tracking. ST loops are based on a decentralized architecture, where the signal tracking and navigation processor of the receiver work independently. Each satellite is independently tracking in separate receiver channels, and they do not share any mutual information between tracking loops/channels. Each channel has its loop filter, whose output provides the corrections to their respective numerically controlled oscillators (NCO). Using the tracked code phase, signal transmission time, and reception time, the code pseudorange measurements are computed. Pseudorange rate measurements are computed based on the estimated Doppler frequency shift. These measurements are then fed to the navigation processor, which calculates the user position, velocity, and timing (PNT) solutions. This approach is the simplest form of receiver architecture. However, due to its decentralized architecture, it does not

exploit the inherent coupling between the dynamics in each channel and the dynamics of the receiver.

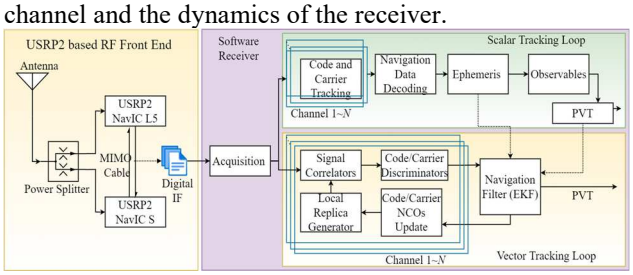

Figure 1. NavIC software receiver architecture with scalar and vector loops.

(b) Vector Tracking or Vectorized NavIC software receiver architecture

Unlike the ST approach, signal tracking and navigation solution determination are no longer separate processes in VT. A single extended Kalman filter (EKF) simultaneously tracks the satellites and estimates the user PNT, thus making it a centralized approach. The phase and frequency of the received signals are predicted from the receivers' estimated PNT. In each channel, residuals are calculated by subtracting the predicted and received signals. These residuals are then used to update the receiver's PNT estimates. Thus, it takes advantage of coupling between the dynamics of individual signals in each channel, and the user dynamics that cause the signals to change are tracked. The most cited benefits of VT are its superior performance in signal challenging conditions, such as low signal strength, ability to reduce noise, and high dynamics [4,6,7].

In this paper, the vector delay frequency lock loop (VDFLL) form has been implemented. VDFLL utilizes the EKF navigation filter to track both the code phase and the carrier frequency of all channels [7]. The vectorized NavIC software receiver presented in this paper is based on the position-state formulation, where the states of the navigation filter are the receiver's position ($\mathbf{X} = [x, y, z]$), velocity ($\mathbf{V} = [v_x, v_y, v_z]$), clock bias ($b$), and clock bias ($\dot{b}$), respectively. The error state vector is expressed as

$$\delta\mathbf{x} = [\delta x\ \delta y\ \delta z\ \delta\dot{x}\ \delta\dot{y}\ \delta\dot{z}\ \delta b\ \delta\dot{b}\ ]^T \quad (1)$$

where $[\ \delta x\ \delta y\ \delta z\ ]^T$ are the errors in user position, $[\delta\dot{x}\ \delta\dot{y}\ \delta\dot{z}\ ]^T$ are the errors in user velocity in the x, y, z coordinates. δb and $\delta\dot{b}$ are the receiver clock bias and drift errors, respectively. The superscript T represents the transpose operator. The NavIC VT loop is initialized by the initial estimates of code phase ($\varphi_{j,k}$), code frequency ($f^j_{code,k}$), carrier frequency ($f^j_{carr,k}$) clock bias (b_k), clock drift ($\dot{b}_k$), and user position ($\mathbf{X}_k$), velocity ($\mathbf{V}_k$), and signal transmit time ($t^j_{tr,k}$) obtained from ST at epoch k. The superscript j represents the jth satellite. To achieve this, ST is activated for the first 50 s (48 s for super frame and 2 s for transient time) so that it acquires and decodes the ephemeris data and consequently compute the navigation solutions used to initialize the vector loop.

The position and velocity are predicted based on the following equations

$$\widehat{\boldsymbol{X}}_{k+1} = \widehat{\boldsymbol{X}}_k + t_{k\to k+1}\boldsymbol{V}_k \quad (2)$$

$$\widehat{\boldsymbol{V}}_{k+1} = \widehat{\boldsymbol{V}}_k \quad (3)$$

where $t_{k\to k+1}$ is the time difference between kth and $k+1$th epoch. Symbol $\widehat{\ }$ represents the estimate of a variable or predicted value. The φ_{k+1}, and $f_{carr,k+1}$, at epoch $k+1$ are predicted based on the predicted user positions/velocities, and satellites positions/velocities from the ephemeris.

$$\hat{\varphi}^j_{k+1} = \varphi^j_k + \left(\Delta\mathbf{X}^j_{k\to k+1} - t_{k\to k+1}\mathbf{V}_k\right)^T \alpha^j_{k+1} + t_{k,k+1}.c \quad (4)$$

$$\hat{f}^j_{code,k+1} = \left[1 + \dot{b}_k + (\mathbf{V}^j_k - \mathbf{V}_k)^T\alpha^j_{k+1}\right]\ f^j_{code,k}/c \quad (5)$$

$$\hat{f}^j_{carr,k+1} = \left[1 + \dot{b}_k + (\mathbf{V}^j_k - \mathbf{V}_k)^T\alpha^j_{k+1}\right]\ f^j_{carr,k}/c \quad (6)$$

where $\Delta\mathrm{X}^j_{k\to k+1}$ is the displacement vector of the jth satellite from epoch k to $k+1$, c is speed of light, α^j_{k+1} is the LOS vector between the receiver and jth satellite. f_{code} is the nominal code frequency (1.023 MHz for C/A code) and f_{carr} is the nominal carrier frequency (L5 = 1176.45 MHz and S = 2492.028 MHz). Based on (1), the state space equation in discrete form can be defined as

$$\delta\mathbf{x}_{k+1} = f(\delta\mathbf{x}_{k+1}) + \mathbf{w}_k;\ \mathbf{w}_k \sim N(0, \mathbf{Q}) \quad (7)$$

$$\boldsymbol{z}_k = h(\delta\mathbf{x}_k) + \mathbf{v}_k;\ \mathbf{v}_k \sim N(0, \mathbf{R}) \quad (8)$$

where $f(.)$ and $h(.)$ are nonlinear functions, w_k and v_k are the process and measurement noises, normally distributed with $\mathbf{Q}$ and $\mathbf{R}$ being their respective co-variance matrices. z_k is the measurement vector given as

$$\boldsymbol{z}_k = [(\Delta\tau^1 \ldots \Delta\tau^M).c/f_{code}\,|\,(\Delta f^1 \ldots \Delta f^M).c/f_{carr}]_{2M\times 1} \quad (9)$$

where M represents the number of satellites. $\Delta\tau^j$ and Δf^j are the code and carrier discriminator outputs from jth satellite, that implicitly contains the pseudorange and pseudorange rate errors. The linear model obtained by linearizing the non-linear functions in (7) and (8) using Jacobian, and estimating the state vector using the expectation operator is

$$\delta\hat{\mathbf{x}}_{k+1} = \mathbf{F}.\delta\hat{\mathbf{x}}_k \quad (10)$$

$$\boldsymbol{z}_k = \mathbf{H}.\delta\hat{\mathbf{x}}_k \quad (11)$$

where $\mathbf{F}$ is the state transition model, and $\mathbf{H}$ is the observation model.

3. Experimental Setup

The performance of the single-frequency (L5/S) ST and VT-based NavIC software receiver are investigated through experimental field tests. Two dynamic field tests were carried out in a semi-urban environment, included one inside the university campus, and one on state highway of Goa. Fig. 2 shows the hardware and software experimental setup used in this work.

Figure 2. Experimental setup. (a) Front-end, (b) receiver, and (c) antenna.

The experimental setup includes the universal software radio peripheral second generation (USRP2)-based RF front-end, and NavIC software receiver processing unit (laptop). Both L5 and S NavIC signals are collected. The

front-end includes two USRP2 devices synced together using a multiple-input and multiple-output (MIMO) cable. The RF front-end was equipped in a car, and the antenna was put on the car's roof. A RF splitter and several cables were used to split the RF signals from the antenna to both USRP2s and the reference hardware (ISRO's in-house IGS) receiver. The sampling frequency and intermediate frequency (IF) of the front-end was set to 4 MHz and 0 MHz, respectively. The collected signals were stored on the laptop through 1 GHz Ethernet.

4. Results and Discussion

The performance is investigated in terms of signal tracking and navigation solutions accuracy. For both dynamic scenarios, seven satellites (PRNs 2, 3, 4, 5, 6, 7 and 9) were visible. Therefore, all satellites were considered for the baseband processing.

(a) Test 1: Dynamic Scenario 1 (Inside University)

The first dynamic scenario was in the university campus, where the trajectory is surrounded by the student hostels and trees. A total of 200 s duration of data was collected, while the car was moving at a speed of 20-25 km/hrs. For the first 50 s the car was in stationary, so that software receiver acquires all satellites, decode the ephemeris and provide the navigation solution. These initial values are used to initialized the VT loop of the receiver.

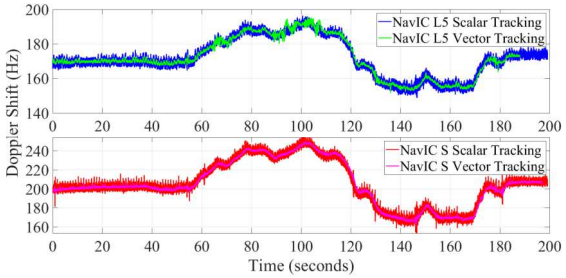

Figure 3. Estimated Doppler shift for dynamic scenario 1 for PRN 4. NavIC L5 (*top*), and NavIC S (*bottom*).

Figure 3 shows the estimated Doppler frequency obtained from the single-frequency (L5/S) ST and VT loops. As can be observed in Fig. 3, the results of ST for both L5 and S are nosier when compared to VT. Both ST and VT can estimate the Doppler frequency. However, the fluctuations in the values of estimated Doppler frequency are quite high in case of ST. Moreover, the ST of S signal shows frequent spikes compared to L5. During, the turns in the path, NavIC L5/S VT keeps the lock and is able to track the smooth changes in the carrier frequency. The velocity solutions of ST and VT for L5 and S are shown in Fig. 4. The velocity solutions of NavIC S ST has huge errors hence not shown in Fig. 4. As can be seen in Fig.4, even the velocity estimates of L5 ST are not smooth hence shows large errors. However, the velocity estimates of VT for both L5 and S were more accurate compared to ST. As velocity estimates of NavIC S ST were not accurate, thus the estimates in VT were also affected. It can be observed that during the turns in the path, the velocity estimates are slight off track. This inaccuracy is possibly due to the signal degradation. The degradation can be because of the high dynamics, and/or nearby interference from 2.45 GHz ISM band wireless devices [6].

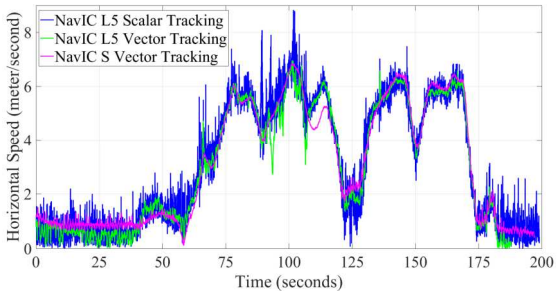

Figure 4. Estimated speed of the vehicle for dynamic scenario 1 using the single-frequency L5/S scalar and vector approaches.

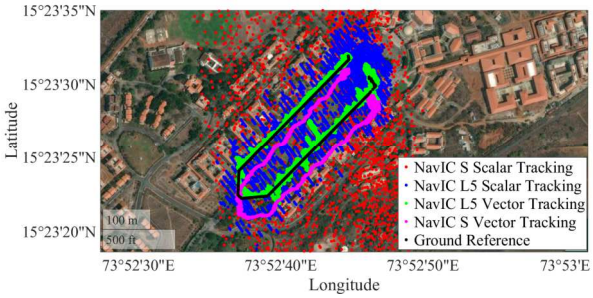

Figure 5. Geoscatter plot of the dynamic scenario 1 tracjectory (from Google Earth).

Figure 5 shows the navigational solutions of the single-frequency (L5/S) ST and VT approaches compared with ground reference visualized on Google Earth. The NavIC L5 VT approach clearly outperforms other approaches. It is consistent with the ground reference and shows smooth variations during the turns in path. It can also be observed in Fig. 5, that the VT solutions for S signals follows the trajectory but with an offset. The navigation solutions of S VT are significantly shifted from the true reference. Similar, variations were observed in S navigation and was reported in [6]. The possible reason for such offset is due to the poor initial estimates of ST that were used to initialize the VT loop. In addition, the degradation in S signal measurements due to high-frequency attenuation and interference could be a potential reason. It is to be noted that, due to degradation in measurements, the ST is unable to estimate proper solutions, as can be seen in the navigation solution of NavIC S ST in Fig. 5. Because of this reason, when VT is initialized with these values takes longer time to converge to minimum error state. This can be clearly be seen in Fig. 5, where the estimates follow the trajectory but not at exact ground reference.

(b) Test 2: Dynamic Scenario 2 (Highway)

The purpose of second dynamic test was to perform the same investigation of ST and VT in location free from nearby obstacle and interference from terrestrial ISM radio band devices. The time and location of the experiment was selected considering the factors that the highway is completely free (to avoid any wireless signal interference) and clear LOS signal is received throughout the signal duration. Fig. 6 shows the estimated Doppler frequency obtained from single (L5/S) ST and VT approaches. It can be observed that the VT approach for both L5 and S is able to estimate the carrier frequency more precisely compared

to ST. Even for the test case 2, the estimates of carrier frequency of ST are nosier, but the receiver is able to track the frequency changes caused by the receiver/satellite dynamics.

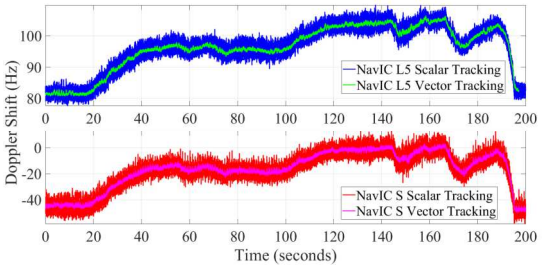

Figure 6. Estimated Doppler shift for dynamic scenario 2 for PRN 6. NavIC L5 (*top*), and NavIC S (*bottom*).

The velocity solutions of ST and VT of L5 and S for dynamic test 2 are shown in Fig. 7. From Fig. 7, it can be observed that the velocity solutions for L5 and S ST are almost equivalent. Obviously, the velocity errors of ST are large compared to VT. But in this case the S ST is far better than the previous test case conducted inside the university campus. Again, the velocity estimates based on vector approach for both L5 and S are smooth and precise.

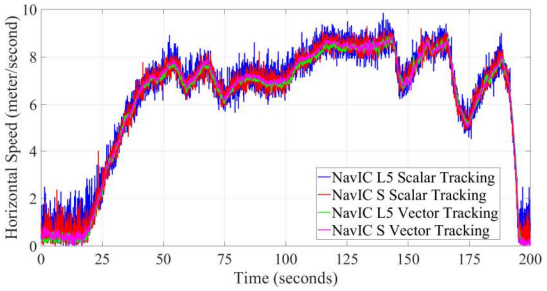

Figure 7. Estimated speed of the vehicle for dynamic scenario 1 using the single-frequency L5/S scalar and vector approaches.

Figure 8 shows the navigational solutions for dynamic scenario 2 of the single-frequency (L5/S) ST and VT approaches compared with ground reference visualized on Google Earth.

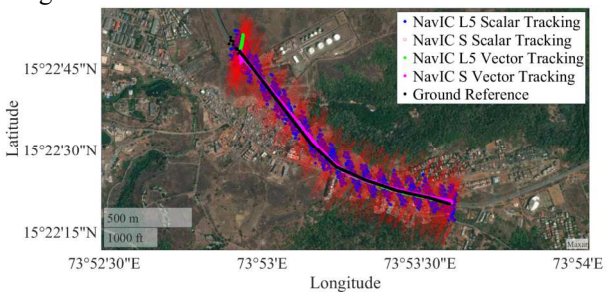

Figure 8. Geoscatter plot of the dynamic scenario 2 tracjectory (from Google Earth).

It can be clearly observed that compared to the dynamic scenario 1, the navigation solutions of NavIC S ST are better. The variations in the ST of S signal are between ± 10 m. Also, the navigation solutions of NavIC S VT are accurate and follow the ground reference. For this test case both L5 and S VT performs equivalent. Additionally, positioning error for the ST of L5 and S are also within the acceptable range of ± 10-15 m. To an extend this analysis confirm that in case of dynamic scenario 1, the NavIC S measurements were possibly affected by the dynamics and especially the interference from ISM band wireless devices. As in dynamic test 2, the whole trajectory was free from any nearby wireless devices operating at 2.45 GHz. Therefore, chances of getting interference from terrestrial devices was negligible, and hence more accurate navigation solutions were obtained.

5. Conclusions

This paper presents an investigation of the performance comparison of single-frequency NavIC ST and VT receiver approach. The performance evaluation was carried out in terms of signal tracking and navigation solution estimation. Two dynamics scenarios were considered for field experiments. The experimental results demonstrated that VT can significantly improve the performance of NavIC software receiver compared to ST. The VT efficiently performs signal tracking and estimates the navigation solution, and velocity. In scenarios with high-dynamics and/or semi-urban environments, VT would be a better approach. In addition, the NavIC S signal measurements are highly affected by the nearby terrestrial wireless devices, which are operating at a frequency close to NavIC S signal bandwidth. Based on the results and conclusion, it is recommended for future work that, if NavIC VT approach is integrated with interference mitigation algorithm then the performance of the receiver could be enhanced in presence of the terrestrial signals.

6. Acknowledgements

This work was financially supported by the Science and Engineering Research Board (SERB) Project under Grant CRG/2021/006784.

7. References

1. Mahato, S., Santra, A., Dan, S., Verma, P., Banerjee, P., & Bose, A. (2020). Visibility anomaly of GNSS satellite and support from regional systems. *Current Science*, *119*(11), 1774-1782.
2. Rao, V. G. (2019, March). NaVIC User Segment Potential, Possibilities and Challenges. In *2019 URSI Asia-Pacific Radio Science Conference (AP-RASC)* (pp. 1-2). IEEE.
3. Jagiwala, D. D., & Shah, S. N. (2018). Impact of Wi-Fi interference on NavIC signal. *Curr Sci*, *114*(11), 2273-2280.
4. Petovello, M. G., O'Driscoll, C., Lachapelle, G., Borio, D., & Murtaza, H. (2008). Architecture and benefits of an advanced GNSS software receiver. *Journal of Global Positioning Systems*, *7*(2), 156-168.
5. Dey, A., Iyer, K., & Sharma, N. (2021, September). S-band interference detection and mitigation using a vector tracking-based NavIC software receiver. In *Proceedings of the 34th International Technical Meeting of the Satellite Division of The Institute of Navigation (ION GNSS+ 2021)* (pp. 3464-3476).
6. Dey, A., Iyer, K., Xu, B., Sharma, N., & Hsu, L. T. (2022). Carrier-Aided Dual-Frequency Vectorized Tracking Architecture for NavIC Signals. *IEEE Transactions on Instrumentation and Measurement*, *71*, 1-13.
7. Zhao, S., & Akos, D. (2011, January). An open source GPS/GNSS vector tracking loop-implementation, filter tuning, and results. In *Proceedings of the 2011 International Technical Meeting of The Institute of Navigation* (pp. 1293-1305).